Transient behavior in single-file systems

Please check the document version of this publication:

• A submitted manuscript is the version of the article upon submission and before peer-review. There can be important differences between the submitted version and the official published version of record. People interested in the research are advised to contact the author for the final version of the publication, or visit the DOI to the publisher's website.
• The final author version and the galley proof are versions of the publication after peer review.
• The final published version features the final layout of the paper including the volume, issue and page numbers.

Link to publication

Transient behavior in single-file systems

S. V. Nedea,[1,*] A. P. J. Jansen,[2] J. J. Lukkien,[1] and P. A. J. Hilbers[3]

[1]*Department of Mathematics and Computing Science, Eindhoven University of Technology, P.O. Box 513, 5600 MB Eindhoven, The Netherlands*
[2]*Department of Chemical Engineering, Eindhoven University of Technology, P.O. Box 513, 5600 MB Eindhoven, The Netherlands*
[3]*Department of Biomedical Engineering, Eindhoven University of Technology, P.O. Box 513, 5600 MB Eindhoven, The Netherlands*
(Received 23 July 2002; published 30 December 2002)

We have used Monte Carlo methods and analytical techniques to investigate the influence of the characteristics, such as pipe length, diffusion, adsorption, desorption, and reaction rates on the transient properties of *single-file systems*. The transient or the relaxation regime is the period in which the system is evolving to equilibrium. We have studied the system when all the sites are reactive and also when only some of them are reactive. Comparisons between mean-field predictions, cluster approximation predictions, and Monte Carlo simulations for the relaxation time of the system are shown. We outline the cases where the mean-field analysis gives good results compared to dynamic Monte Carlo results. For some specific cases we can analytically derive the relaxation time. Occupancy profiles for different distributions of the sites both for the mean field and simulations are compared. Different results for slow and fast reaction systems and different distributions of reactive sites are discussed.

PACS number(s): 02.70.Uu, 02.60.−x, 05.50.+q, 07.05.Tp

I. INTRODUCTION

Although systems in nature evolve by obeying physical laws, it is in most cases difficult or not feasible to describe the system properties accurately since details of the microscopic dynamics are not fully known. Therefore we usually deal with simplified models for these systems, of which stochastic models are an example. They are thus described by a reduced set of dynamic variables. Although many exact solutions have been found [1–6], the vast majority of stochastic models cannot be solved exactly. Many results for equilibrium systems [7–11] have been classified. In nature, however, equilibrium is rather an exception than a rule. In most cases the temporal evolution starts from an initial state that is far away from equilibrium. The relaxation of such a system towards its stationary state depends on the specific dynamical properties and cannot be described within the framework of equilibrium statistical mechanics. Instead, it is necessary to set up a model for the microscopic dynamics of the system. Assuming certain transition probabilities, the time-dependent probability distribution $P_t(s)$ to find the system in configuration s has to be derived from the master equation (ME). Solving the ME is usually a difficult task. Therefore, the theoretical understanding of nonequilibrium processes is still at its beginning. Better understanding of these phenomena would be an important step as nonequilibrium systems exhibit a richer behavior than equilibrium systems [12–16].

We investigate nonequilibrium processes for a *single-file system* (SFS) with conversion. In Ref. [17] we have already elaborated on the special properties of porous structures such as zeolites. The one-dimensional nature of the zeolite channel leads to extraordinary effects on the kinetic properties of these materials. These structures are modeled by one-dimensional systems called single-file Systems where particles are not able to pass each other. In Ref. [17] we have focused on the steady-state properties of a SFS with conversion. The process of diffusion in SFS has different characteristics as ordinary diffusion, which affects the nature of both transport and conversion by chemical reactions. We are investigating the kinetic properties of this system, and, more precisely, we are interested in the properties of the system before reaching equilibrium (the transient or relaxation regime).

Different methods and techniques have been described in the literature to solve the ME exactly [8,12,18]. In spite of the remarkable progress in the field of exactly solvable nonequilibrium processes, the majority of reaction-diffusion models cannot be solved exactly [19,20]. It is therefore necessary to use approximation techniques in order to describe their essential properties [e.g., mean-field (MF) approximation, cluster approximation] [21]. Also, as was already realized by Smoluchowski [22], fluctuations and correlations may be extremely important in low-dimensional systems where the diffusive mixing is not strong. Therefore, these approximation techniques can give results that deviate strongly from the system behavior. Dynamic Monte Carlo (DMC) methods are used to simulate the system according to the ME.

Few researchers have concentrated on the properties of the system in the transient regime and only studied the reactivity of the system in this regime. Moreover, little research has been done for an open system where adsorption (desorption) is present at the marginal sites. The reason that many of the analytical approaches fail is because of the asymmetry of the system.

In the present work we focus on the nonequilibrium phase properties of SFS with conversion. We study the relaxation time of the system (time evolution of the system properties, starting with no particles) for different sets of kinetic parameters, lengths of the pipe, and distributions of the reactive

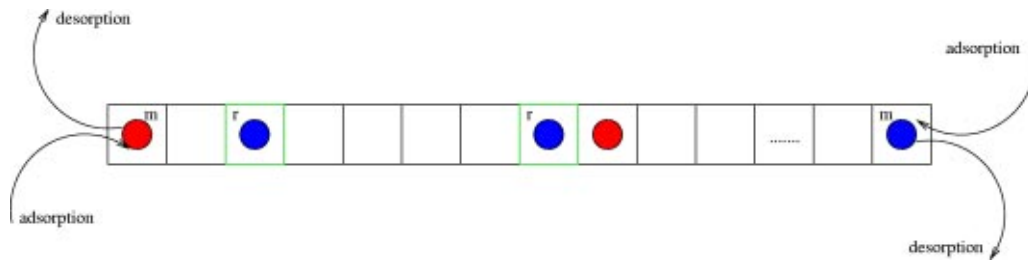*Electronic address: silvia@win.tue.nl

FIG. 1. Picture of a single-file system with two types of adsorbed particles.

sites. In the transient regime we observe that the MF results are close to the DMC results both for slow and fast reaction systems. We outline the cases for which the differences are significant. We compare with the steady-state situation in which the MF was not describing the single-file effects properly [17]. We analyze the situations when analytical results can be derived, and we compare these results with the MF and DMC results. We look at the relaxation of the total loading, loading with different components, occupancies of individual sites for various parameters, and different distributions of the reactive sites. As MF is a coarse approximation, for the analysis of profile occupancies we introduce a better approximation (cluster approximation). We analyze the results using different analytic methods such as pair and MF approximation. Pair approximation and MF approximation tend to give similar results due to the high-order correlations in the system. We investigate the effect of various model assumptions made about diffusion, adsorption, desorption, and reaction on the kinetic behavior of the system.

In Sec. II we specify our mathematical model together with the theoretical background for analytical and simulation results. In Sec. III A we present the various results for transient regimes for the simplified model without conversion. We solve numerically and analytically the master equation in order to get the relaxation time of the system. In Sec. III B we use the MF theory to simplify the rate equations [17] of the system for the case when all the sites have the same activity towards conversion. We present the results obtained using DMC simulations for the case with conversion when all the sites are reactive in Sec. III C 1, and when only some of the sites are reactive in Sec. III C 2. For all these cases we compare the DMC results with the MF and pair approximation results. The influence of the position of the reactive sites is also outlined. The last section summarizes our main conclusions.

II. THEORY

In this section we give the theoretical background for our analytical and simulation results. First we specify our model and then we show that the defined system obeys a ME. We derive then a set of exact rate equations from the master equation of the system describing the reaction kinetics. We look at the properties of the system in the transient regime by solving these rate equations. In order to do this we have to use approximation techniques. We use the MF analysis and derive a set of equations that we can solve numerically. Because MF is a strong simplification and neglects all spatial correlations in the system, we introduce another approximation called the cluster approximation. We have also simulated the system governed by the ME using DMC simulations.

A. The model

We model a single-file system by a one-dimensional array of sites, each possibly occupied by an adsorbate (see Fig. 1). This is the model of diffusion and reaction in a one-dimensional arrangement of particles with hard-core interaction. The sites are numbered $1, 2, \ldots, S$. A particle can only move to the right or to the left if an adjacent site is vacant. The sites could be reactive and unreactive and we note with N_{prot} the number of reactive sites. A reactive site is the only place where a conversion may take place.

We consider two types of adsorbates, A and B, in our model and we denote with Y the site occupation of a site, $Y = (*, A, B)$, which stands for a vacant site, a site occupied by A, or a site occupied by a B, respectively. We restrict ourselves to the following monomolecular and bimolecular transitions.

1. Adsorption and desorption

Adsorption and desorption take place only at the two marginal sites, i.e., the left and rightmost sites at the ends of the system:

$$A(\text{gas}) + *_m \rightarrow A_m,$$

$$A_m \rightarrow A(\text{gas}) + *_m,$$

$$B_m \rightarrow B(\text{gas}) + *_m,$$
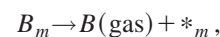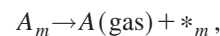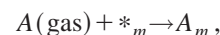
where subscript m denotes a marginal site. Note that there is no B adsorption. B's can only be formed by conversion.

2. Diffusion

In the pipe, particles are allowed to diffuse via hopping to vacant nearest neighbor sites:

$$A_n + *_{n+1} \leftrightarrow *_n + A_{n+1},$$

$$B_n + *_{n+1} \leftrightarrow *_n + B_{n+1},$$
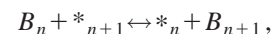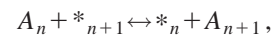
where the subscripts are site indices; $n = 1, 2, \ldots, S-1$.

3. Conversion

An A can transform into a B at a reactive site:

$$A_r \rightarrow B_r.$$
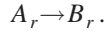
In the initial state of the system all the sites are vacant (no particles in the pipe) as we are interested in the behavior of the system towards equilibrium.

B. Master equation

Reaction kinetics is described by a stochastic process. Every reaction has a microscopic rate constant associated with it that is the probability per unit time that the reaction occurs. Stochastic models of physical systems can be described by a master equation [23].

By α, β, we will indicate a particular configuration of the system, i.e., a particular way to distribute adsorbates over all the sites. $P_\alpha(t)$ will indicate the probability of finding the system in configuration α at time t and $W_{\alpha\beta}$ is the rate constant of the reaction changing configuration β to configuration α.

The probability of the system being in configuration α at time $t+dt$ can be expressed as the sum of two terms. The first term is the probability to find the system already in configuration α at time t multiplied by the probability to stay in this configuration during dt. The second term is the probability to find the system in some other configuration β at time t multiplied by the probability to go from β to α during dt:

$$P_\alpha(t+dt) = \left(1 - dt \sum_\beta W_{\beta\alpha}\right) P_\alpha(t) + dt \sum_\beta W_{\alpha\beta} P_\beta(t).$$
(1)

By taking the limit $dt \rightarrow 0$ this equation reduces to a master equation:

$$\frac{dP_\alpha(t)}{dt} = \sum_\beta [W_{\alpha\beta} P_\beta(t) - W_{\beta\alpha} P_\alpha(t)].$$
(2)

Analytical results can be derived as follows. The value of a property X is a weighted average over the values X_α which is the value of X in configuration α,

$$\langle X \rangle = \sum_\alpha P_\alpha X_\alpha.$$
(3)

From this follows the rate equation:

$$\frac{d\langle X \rangle}{dt} = \sum_\alpha \frac{dP_\alpha}{dt} X_\alpha = \sum_{\alpha\beta} [W_{\alpha\beta} P_\beta - W_{\beta\alpha} P_\alpha] X_\alpha$$

$$= \sum_{\alpha\beta} W_{\alpha\beta} P_\beta (X_\alpha - X_\beta).$$
(4)

C. Analytical methods

1. Rate equations

Starting from the master equation (2) and using expression (4) the rate equations of the system are derived [17]. We denote by W_{ads}, W_{des}, W_{diff}, W_{rx} the rate constants of adsorption, desorption, diffusion, and conversion, respectively. For simplicity we assume that the rate constants of A and B desorption are equal, and also the rate constants of A and B diffusion are equal. We denote by $\langle Y_n \rangle$ the probability that a particle of type Y is on site n, and with $\langle Y_n Y_{n+1} \rangle$ the probability that a particle of type Y is at site n and one at site $n+1$, where $Y=(*,A,B)$. The coefficients Δ_n, where $n=1,2,\ldots,S$, are 1 if site n is reactive and 0 otherwise. The rate equations for a nonmarginal site are

$$\frac{d\langle A_n \rangle}{dt} = W_{diff}[-\langle A_n *_{n+1} \rangle$$
$$- \langle A_n *_{n-1} \rangle + \langle A_{n-1} *_n \rangle + \langle A_n *_{n+1} \rangle] - \Delta_n W_{rx} \langle A_n \rangle.$$
(5)

For $\langle B_n \rangle$ we get similarly

$$\frac{d\langle B_n \rangle}{dt} = W_{diff}[-\langle B_n *_{n+1} \rangle - \langle *_{n-1} B_n \rangle + \langle B_{n-1} *_n \rangle$$
$$+ \langle *_n B_{n+1} \rangle] + \Delta_n W_{rx} \langle A_n \rangle.$$
(6)

The marginal sites also have adsorption and desorption. They can be dealt with similary as the conversion. The rate equations for A are

$$\frac{d\langle A_1 \rangle}{dt} = W_{diff}[-\langle A_1 *_2 \rangle + \langle *_1 A_2 \rangle] + W_{ads} \langle *_1 \rangle - W_{des} \langle A_1 \rangle$$
$$- \Delta_1 W_{rx} \langle A_1 \rangle,$$

$$\frac{d\langle A_S \rangle}{dt} = W_{diff}[-\langle *_{S-1} A_S \rangle + \langle A_{S-1} *_S \rangle] + W_{ads} \langle *_S \rangle$$
$$- W_{des} \langle A_S \rangle - \Delta_S W_{rx} \langle A_S \rangle,$$
(7)

and the rate equations for B are

$$\frac{d\langle B_1 \rangle}{dt} = W_{diff}[-\langle B_1 *_2 \rangle + \langle *_1 B_2 \rangle] - W_{des} \langle B_1 \rangle + \Delta_1 W_{rx} \langle A_1 \rangle,$$

$$\frac{d\langle B_S \rangle}{dt} = W_{diff}[-\langle *_{S-1} B_S \rangle + \langle B_{S-1} *_S \rangle] - W_{des} \langle B_1 \rangle$$
$$+ \Delta_S W_{rx} \langle A_S \rangle.$$
(8)

Note that these coupled sets of differential equations are exact, but not closed.

2. Mean field

To solve this coupled set of differential equations, we need to make an approximation for the two-site probabilities such as $\langle A_n *_{n+1} \rangle$, $\langle B_n *_{n+1} \rangle$, etc. The closure relation

$$\langle X \rangle = \sum_Y \langle XY \rangle \qquad (9)$$

should hold for any approximation for these two-site probabilities. We denote with X the occupation of site n and with Y the occupation of site $n+1$. The simplest approximation is

$$\langle XY \rangle = \langle X \rangle \langle Y \rangle, \qquad (10)$$

i.e., neighboring sites are considered independent.

The two-site probabilities then become $\langle A_n *_{n+1} \rangle = \langle A_n \rangle \times \langle *_{n+1} \rangle$, $\langle B_n *_{n+1} \rangle = \langle B_n \rangle \langle *_{n+1} \rangle$ [21]. This approximation is called the mean-field approximation and gives us a coupled set of differential equations that we can solve numerically.

3. Cluster approximation

The MF approximation is a strong simplification because it neglects all spatial correlations in the system. Because the system we analyze is onedimensional, the correlations might be significant and important. The obvious possibility to eliminate the weakness of the MF approach is to introduce another approximation.

Instead of using the MF approximation for the two-site probabilities, we write down their rate equations (see the Appendix). These equations have three-site probabilities, which we approximate. This leads to a so-called cluster approximation. The closure relation

$$\langle XY \rangle = \sum_Z \langle XYZ \rangle \qquad (11)$$

should now hold for any approximation. We denote here with X the occupation of site n, with Y the occupation of site $n+1$, and with Z the occupation of site $n+2$.

There are various decoupling schemes used in the literature [2,4,6,18,24] as approximations for the n-site probabilities. For many of these decoupling schemes the closure relation (11) no longer holds. For simplicity we will use the simplest cluster approximation, called pair approximation, for which only the correlations between pairs of nearest neighbors (NN) are considered.

The decoupling scheme for our pair approximation is

$$\langle XYZ \rangle = \frac{\langle XY \rangle \langle YZ \rangle}{\langle Y \rangle}. \qquad (12)$$

It is straightforward to see that the closure relation (11) holds:

$$\sum_Z \langle XYZ \rangle = \frac{\langle XY \rangle}{\langle Y \rangle} \sum_Z \langle YZ \rangle = \frac{1}{\langle Y \rangle} \langle XY \rangle \langle Y \rangle = \langle XY \rangle. \qquad (13)$$

After decoupling, this system of coupled sets of differential equations, consisting of the rate equations for one-site and two-site probabilities, becomes closed and can be solved numerically.

D. Dynamic Monte Carlo

We have seen that we can derive approximate analytical solutions to the master equation. DMC methods allow us to simulate the system governed by the master equation over time. We simplify the notation of the master equation by defining a matrix **W** containing the rate constants $W_{\alpha\beta}$, and a diagonal matrix **R** by $R_{\alpha\beta} \equiv \sum_\gamma W_{\gamma\beta}$, if $\alpha = \beta$, and 0 otherwise. If we put the probabilities of the configurations P_α in a vector **P**, we can write the master equation as

$$\frac{d\mathbf{P}}{dt} = -(\mathbf{R} - \mathbf{W})\mathbf{P}, \qquad (14)$$

where **R** and **W** are time independent. We also introduce a new matrix **Q**, $\mathbf{Q}(t) \equiv \exp(-\mathbf{R}t)$. This matrix is time dependent by definition and we can rewrite the master equation in the integral form

$$\mathbf{P}(t) = \mathbf{Q}(t)\mathbf{P}(0) + \int_0^t dt' \mathbf{Q}(t-t')\mathbf{W}\mathbf{P}(t'). \qquad (15)$$

By substitution, we get from the right-hand side for $\mathbf{P}(t')$,

$$\mathbf{P}(t) = \left[\mathbf{Q}(t) + \int_0^t dt' \mathbf{Q}(t-t')\mathbf{W}\mathbf{Q}(t') + \int_0^t dt' \int_0^{t'} dt'' \mathbf{Q}(t - t')\mathbf{W}\mathbf{Q}(t'-t'')\mathbf{W}\mathbf{Q}(t'') + \cdots \right] \mathbf{P}(0). \qquad (16)$$

Suppose at $t=0$ the system is in configuration α with probability $P_\alpha(0)$. The probability that, at time t, the system is still in configuration α is given by $Q_{\alpha\alpha}(t)P_\alpha(0) = \exp(-R_{\alpha\alpha}t)P_\alpha(0)$. This shows that the first term represents the contribution to the probabilities when no reaction takes place up to time t. The matrix **W** determines how the probabilities change when a reaction takes place. The second term represents the contribution to the probabilities when no reaction takes place between times 0 and t', some reaction takes place at time t', and then no reaction takes place between t' and t. The subsequent terms represent contributions when two, three, four, etc. reactions take place. The idea of the DMC method is not to compute probabilities $P_\alpha(t)$ explicitly, but to start with some particular configuration, representative for the initial state of the experiment one wants to simulate, and then generate a sequence of other configurations with the correct probability. The method generates a time t' when the first reaction occurs according to the probability distribution $1 - \exp(-R_{\alpha\alpha}t)$. At time t' a reaction takes place such that a new configuration α' is generated by picking it out of all possible new configurations β with a probability proportional to $W_{\alpha'\alpha}$. At this point we can proceed by repeating the previous steps, drawing again a time for a new reaction and a new configuration [25–47].

III. RESULTS AND DISCUSSION

In Ref. [17] various results for the system with conversion ($W_{rx} \neq 0$) and without conversion ($W_{rx} = 0$) were reported. In case $W_{rx} = 0$ we have only A particles in the system. The

total loading Q of the system is defined as the average number of particles per site. In case $W_{rx} \neq 0$ we have B's as well in the system. In this case, the total loading Q, is the sum of the loading with A particles (Q_A) and loading with B particles (Q_B)

$$Q = \frac{1}{S}\sum_{n=1}^{S}\langle A_n\rangle + \frac{1}{S}\sum_{n=1}^{S}\langle B_n\rangle. \tag{17}$$

Note that the total loading of the pipe for the model with conversion is the same as for the model without conversion [17]. We study the relaxation time of the system without conversion and of the system with conversion.

A. No conversion

We are interested in the relaxation time of the system (transients). We start with the evolution of the total loading over time starting from a system with no particles at all. As the total loading is the same for the case with and without conversion, we will consider, for simplicity, the case with no conversion first.

As we can derive a finite set of exact rate equations (5)–(8) it's not necessary to work with the master equation in this case. With $\langle X_n\rangle$ the probability that site n is occupied, we have

$$\frac{d\langle X_n\rangle}{dt} = W_{diff}[-\langle X_n *_{n+1}\rangle - \langle_{n-1}*X_n\rangle + \langle X_{n-1}*_n\rangle$$

$$+ \langle *_n X_{n+1}\rangle] \tag{18}$$

when n is not a marginal site. The two-site probabilities can be eliminated by using closure relations,

$$\langle X_n X_{n+1}\rangle + \langle X_n *_{n+1}\rangle = \langle X_n\rangle, \tag{19}$$

that hold in this specific case. The probabilities with particles on both neighboring sites cancel and the result is

$$\frac{d\langle X_n\rangle}{dt} = W_{diff}[\langle X_{n-1}\rangle - 2\langle X_n\rangle + \langle X_{n+1}\rangle]. \tag{20}$$

For the marginal sites we get

$$\frac{d\langle X_1\rangle}{dt} = W_{ads}[1 - \langle X_1\rangle] - W_{des}\langle X_1\rangle + W_{diff}[\langle X_2\rangle - \langle X_1\rangle]$$

and

$$\frac{d\langle X_S\rangle}{dt} = W_{ads}[1 - \langle X_S\rangle] - W_{des}\langle X_S\rangle + W_{diff}[\langle X_{S-1}\rangle - \langle X_S\rangle]. \tag{21}$$

These equations are used for the derivation of the relaxation time. The rate equations are going to be simplified to a point where they are a set of homogeneous linear ordinary differential equations (ODE's) with only one parameter apart from the system size. Dividing by $W_{ads} + W_{des}$ and introducing the dimensionless parameters

$$\langle X_{eq}\rangle \equiv \frac{W_{ads}}{W_{ads} + W_{des}},$$

$$\lambda \equiv \frac{W_{diff}}{W_{ads} + W_{des}},$$

$$\tau \equiv (W_{ads} + W_{des})t, \tag{22}$$

we get

$$\frac{d\langle X_1\rangle}{d\tau} = \langle X_{eq}\rangle - \langle X_1\rangle + \lambda[\langle X_2\rangle - \langle X_1\rangle],$$

$$\frac{d\langle X_n\rangle}{d\tau} = \lambda[\langle X_{n-1}\rangle - 2\langle X_n\rangle + \langle X_{n+1}\rangle],$$

$$\frac{d\langle X_S\rangle}{d\tau} = \langle X_{eq}\rangle - \langle X_S\rangle + \lambda[\langle X_{S-1}\rangle - \langle X_S\rangle]. \tag{23}$$

We can write these equations in matrix-vector notation as

$$\frac{d\langle \mathbf{X}\rangle}{d\tau} = -\mathbf{M}\langle \mathbf{X}\rangle + \mathbf{v}, \tag{24}$$

where $\langle \mathbf{X}\rangle$ is a vector containing the occupancy probabilities, $\mathbf{M}$ is the matrix of coefficients having the form

$$\begin{pmatrix}
1+\lambda & -\lambda & 0 & 0 & \cdots & & & & & \\
-\lambda & 2\lambda & -\lambda & 0 & \cdots & & & & & \\
0 & -\lambda & 2\lambda & -\lambda & & & & & & \\
0 & 0 & -\lambda & 2\lambda & \ddots & & & & & \\
\vdots & \vdots & & & \ddots & \ddots & \ddots & & \vdots & \vdots \\
& & & & \ddots & 2\lambda & -\lambda & 0 & 0 \\
& & & & & -\lambda & 2\lambda & -\lambda & 0 \\
& & & \cdots & & 0 & -\lambda & 2\lambda & -\lambda \\
& & & \cdots & & 0 & 0 & -\lambda & 1+\lambda
\end{pmatrix} \tag{25}$$

and **v** is the vector that makes the system nonhomogeneous. The parameter $\langle X_{eq} \rangle$ is the equilibrium coverage.

Finally we can make the set of equations homogeneous by working with probabilities for vacancies: i.e., with

$$\mathbf{y} \equiv 1 - \frac{\langle \mathbf{X} \rangle}{\langle X_{eq} \rangle} \tag{26}$$

we get

$$-\frac{d\mathbf{y}}{d\tau} = \mathbf{My}. \tag{27}$$

In order to solve Eq. (27), we try the substitution

$$\mathbf{y} = \mathbf{a} e^{-\omega\tau}. \tag{28}$$

Taking out the exponential leaves us with

$$\mathbf{Ma} = \omega \mathbf{a}. \tag{29}$$

Removing the time dependence yields relaxation times. We see that we have obtained an eigenvalue equation. The eigenvalues ω are the reciprocals of relaxation times for the corresponding eigenvectors. The relaxation time of the system as a whole (t_{rel}) is the reciprocal of the smallest eigenvalue. We can get this time by simply numerically solving the eigenvalue equation for given S and λ.

1. Solving the eigenvalue equation analytically

For some special cases analytical expressions for the eigenvalues can be given. We consider the ansatz

$$a_n = z^n. \tag{30}$$

If we substitute a_n from expression (29) into the equation for n not a marginal site, we get

$$\lambda \left[-\frac{1}{z} + 2 - z \right] = \omega. \tag{31}$$

This equation has two solutions.

$$z_{\pm} = 1 - \tfrac{1}{2}f \pm \tfrac{1}{2}\sqrt{f^2 - 4f}, \tag{32}$$

where

$$f \equiv \frac{\omega}{\lambda}. \tag{33}$$

There are two cases to be distinguished. If $f \geq 4$, then both solutions are real. Because this is the same as $\omega \geq 4\lambda$, we will have this for slow diffusion and for eigenvectors with fast relaxation (large ω). As we are interested in the slowest relaxation (small ω) we will look at the other case $f < 4$ or $\omega < 4\lambda$. The two solutions are then each others' complex conjugate. (Note for the following that $f \geq 0$.)

2. Fast diffusion or slow relaxation

In this case we can write the solutions as

$$z_{\pm} = r e^{\pm i\varphi}, \tag{34}$$

where r and φ are both real. In fact the equation for z shows that when z is a solution, then so is $1/z$. This means that $r = 1$, or

$$z_{\pm} = e^{\pm i\varphi}. \tag{35}$$

Substitution in the equation for z yields

$$\cos\varphi = 1 - \tfrac{1}{2}f. \tag{36}$$

This has indeed only solutions for $0 \leq f \leq 4$.

Because there are two solutions for z, the solution for a_n is a linear combination of these two solutions: i.e.,

$$a_n = c_1 e^{in\varphi} + c_2 e^{-in\varphi}. \tag{37}$$

From Eq. (28) we remark that a_n should be always real. This means that c_1 is the complex conjugate of c_2. The coefficients will follow from the equations for the marginal sites. There are two of these equations. The equation above for $\cos\varphi$ is a third equation. We have four unknowns (c_1, c_2, ω, and φ), but, as only the ratio between the coefficients can be determined, we should effectively be able to determine all of them.

Substitution of the expression for a_n in the equations for the marginal sites, taking into account that c_1 and c_2 are complex conjugate ($c_1 = c_{1R} + i c_{1I}$), leads to

$$\begin{pmatrix} 2(1-\omega+\lambda)\cos(\varphi) - 2\lambda\cos(2\varphi) & -2\sin(\varphi)(1-\omega+\lambda) + 2\lambda\sin(2\varphi) \\ 2\cos(S\varphi)(1-\omega+\lambda) - 2\lambda\cos[(S-1)\varphi] & -2(1-\omega+\lambda)\sin(S\varphi) + 2\lambda\sin[(S-1)\varphi] \end{pmatrix} \begin{pmatrix} c_{1R} \\ c_{1I} \end{pmatrix} = \begin{pmatrix} 0 \\ 0 \end{pmatrix}. \tag{38}$$

This equation only has nontrivial solutions (the trivial solution is $c_{1R} = c_{1I} = 0$) when the determinant of the matrix equals zero. This leads to the following equation:

$$8\lambda(-\omega+\lambda+1)\sin[(S-2)\varphi] - 4(-\omega+\lambda+1)^2\sin[(S-1)\varphi] + 4\lambda^2\sin[(S-3)\varphi] = 0. \tag{39}$$

We can eliminate ω by using $\cos\varphi = 1 - f/2$.

Using φ as parameter in Eq. (39), $\varphi \in [0,\pi]$, we can get the λ's. Equations (35) and (32) gives us the ω's. We get in this way ω as a function of λ, coupled by the parameter φ (see Fig. 2).
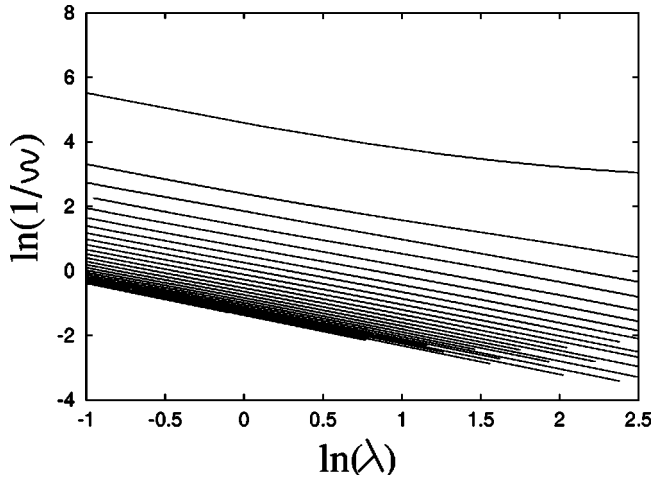
FIG. 2. The general solution for $\ln(1/\omega)$ as a function of $\ln(\lambda)$, for $\varphi \in [0, \pi)$, and $S = 30$.

3. Solving the eigenvalue equation for the total loading, in the case $\lambda \to \infty$

We solve the eigenvalue equation numerically in order to get the relaxation time of a system. We want to describe how the relaxation time of the total loading (t_{rel}) depends on system parameters such as reaction, adsorption (desorption), diffusion rate constants, and system size S. In Fig. 2 we show the influence of diffusion on the relaxation time for a system of size $S = 30$. Note that there are two regimes describing the dependence on diffusion of the relaxation time t_{rel}. The first regime is for slow diffusion, when t_{rel} decreases rapidly with increasing diffusion, and the second for fast diffusion, when t_{rel} slowly decreases with diffusion to a limiting value.

Because diffusion is infinitely fast, all the sites have the same probability to be occupied and the system is homogeneous. We can then analytically derive the limiting value of t_{rel} for infinitely fast diffusion from the equation

$$\frac{d\langle X_n \rangle}{dt} = \frac{2W_{ads}}{S}[1 - \langle X_n \rangle] - \frac{2W_{des}}{S}\langle X_n \rangle. \quad (40)$$

The first term is the probability of a particle to be adsorbed at the two open ends, and the second is the probability of a particle to be desorbed at the two open ends. The probability of a particle to be adsorbed to one end equals the adsorption rate constant W_{ads} times the probability to have there a vacancy $(1 - \langle X_n \rangle)$, while the probability of a particle to be desorbed equals the desorption rate constant W_{des} times the probability to have a particle ($\langle X_n \rangle$).

From the above equation we get the expression for $\langle X_n \rangle$,

$$\langle X_n \rangle = \langle X_{eq} \rangle \left[1 - \exp\left(\frac{-2(W_{ads} + W_{des})}{S} t \right) \right]. \quad (41)$$

The relaxation time is
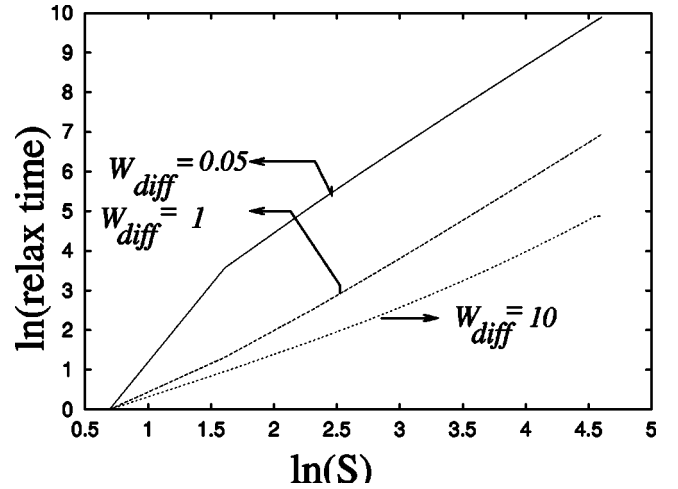
$$t_{rel} = \frac{S}{2(W_{ads} + W_{des})}. \quad (42)$$

FIG. 3. The logarithm of the relaxation time as a function of $\ln(S)$ for the parameters $W_{ads} = 0.2$, $W_{des} = 0.8$, and different W_{diff}.

This limiting value is the same as the one indicated by the convergence of the curves in Fig. 2. The other parameter that influences the relaxation time t_{rel} is the length of the pipe S. For diffusion very fast, t_{rel} increases linearly with S (see Fig. 3).

B. Conversion

In the case with no conversion, we have derived a set of exact equations and we have simplified the rate equations to homogeneous linear ODE's. Including conversion in our model, the two-site probabilities cannot be eliminated and an approximation is needed. We use the MF approximation and we get a coupled set of differential equations that we can solve numerically. In Fig. 4, from the MF results for the transients, we observe that there are two different behaviors determined by conversion.

For fast reaction systems [see Fig. 4(a)], the relaxation time of the loading with A's (t_{relA}) and B's (t_{relB}) is equal to the relaxation time of the total loading (t_{rel}). This means that when Q has reached equilibrium, Q_A and Q_B have also reached equilibrium.

For slow reaction systems [see Fig. 4(b)], the total loading Q relaxes faster to equilibrium than the loading with A's (Q_A) and B's (Q_B). The regime between Q reaching equilibrium and Q_A and Q_B reaching equilibrium we call the reaction limited regime.

We remark that for slow reaction systems in the reaction limited regime, the vacancy probability can be replaced with the steady-state expression $\langle *_n \rangle = W_{des}/(W_{ads} + W_{des})$. The set of equations for the case when all the sites are reactive then becomes

$$\frac{d\langle A_n \rangle}{dt} = \frac{W_{diff}W_{des}}{W_{ads} + W_{des}}[\langle A_{n+1} \rangle + \langle A_{n-1} \rangle - 2\langle A_n \rangle] - W_{rx}\langle A_n \rangle,$$

$$\frac{d\langle B_n \rangle}{dt} = \frac{W_{diff}W_{des}}{W_{ads} + W_{des}}[\langle B_{n+1} \rangle + \langle B_{n-1} \rangle - 2\langle B_n \rangle] + W_{rx}\langle A_n \rangle,$$
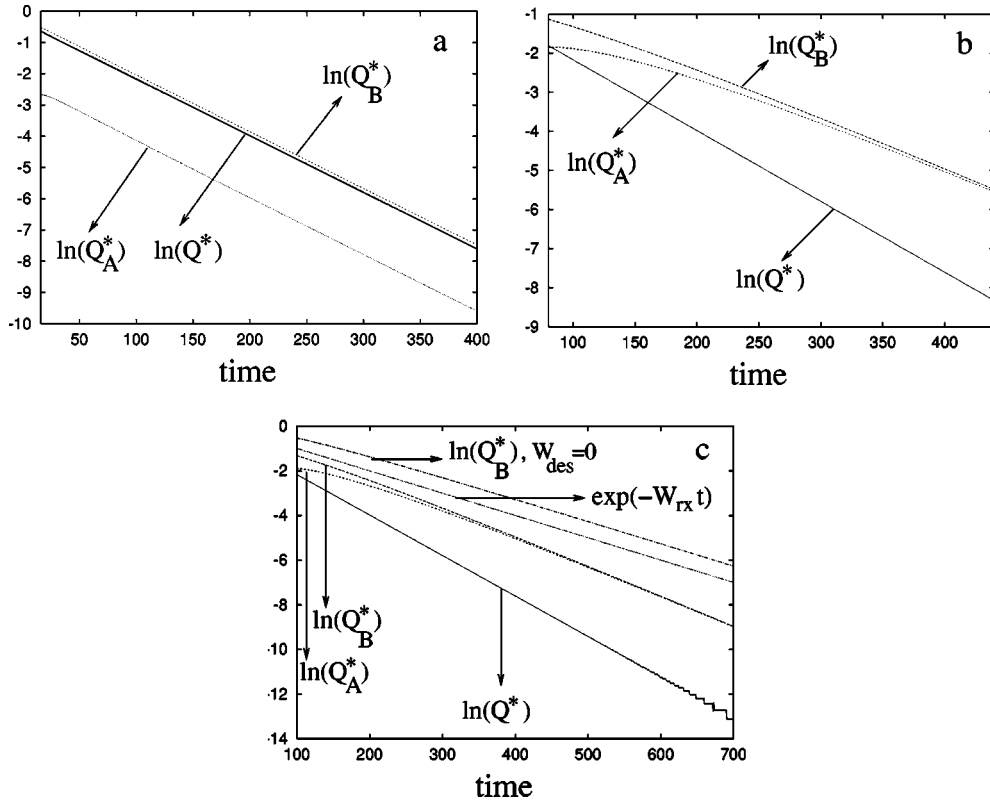
FIG. 4. (a) Time dependence of $\ln(Q^*)$, $\ln(Q_A^*)$, and $\ln(Q_B^*)$ for fast reaction systems ($W_{\text{ads}}=0.8, W_{\text{des}}=0.2, W_{\text{diff}}=1; W_{\text{rx}}=2$). (b) Time dependence of the $\ln(Q^*)$, $\ln(Q_A^*)$ and $\ln(Q_B^*)$ for slow reaction systems ($W_{\text{ads}}=0.8, W_{\text{des}}=0.2, W_{\text{diff}}=2; W_{\text{rx}}=0.01$). (c) Comparison between time dependence of $\ln(Q^*)$, $\ln(Q_A^*)$, $\ln(Q_B^*)$ and the time dependence of the function $\exp(-W_{\text{rx}}^*t)$. For slow reaction systems, the slope depends only on W_{rx}, but also on desorption. We have marked the time dependence of the $\ln(Q_B^*)$ when $W_{\text{des}}=0$. In (a)–(c) we have marked with * the absolute value of the difference between the current value and the steady-state value of the parameter.

$$\frac{d\langle A_1 \rangle}{dt} = \frac{W_{\text{diff}}W_{\text{des}}}{W_{\text{ads}}+W_{\text{des}}}[\langle A_2 \rangle - \langle A_1 \rangle] - W_{\text{rx}}\langle A_1 \rangle$$

$$- W_{\text{des}}\langle A_1 \rangle + \frac{W_{\text{ads}}W_{\text{des}}}{W_{\text{ads}}+W_{\text{des}}},$$

$$\frac{d\langle B_1 \rangle}{dt} = \frac{W_{\text{diff}}W_{\text{des}}}{W_{\text{ads}}+W_{\text{des}}}[\langle B_2 \rangle - \langle B_1 \rangle] + W_{\text{rx}}\langle A_1 \rangle - W_{\text{des}}\langle B_1 \rangle,$$

$$\frac{d\langle A_S \rangle}{dt} = \frac{W_{\text{diff}}W_{\text{des}}}{W_{\text{ads}}+W_{\text{des}}}[\langle A_{S-1} \rangle - \langle A_S \rangle] - W_{\text{rx}}\langle A_S \rangle$$

$$- W_{\text{des}}\langle A_S \rangle + \frac{W_{\text{ads}}W_{\text{des}}}{W_{\text{ads}}+W_{\text{des}}},$$

$$\frac{d\langle B_S \rangle}{dt} = \frac{W_{\text{diff}}W_{\text{des}}}{W_{\text{ads}}+W_{\text{des}}}[\langle B_{S-1} \rangle - \langle B_S \rangle] + W_{\text{rx}}\langle A_S \rangle - W_{\text{des}}\langle B_S \rangle.$$

$$(43)$$

We can use these approximate MF equations for the problem of relaxation of A and B loadings for the case when the total loading has already reached a steady state. The equations for A's can be written as

$$\frac{d\langle \mathbf{A} \rangle}{dt} = \mathbf{M}'\langle \mathbf{A} \rangle + \mathbf{v}', \qquad (44)$$

where $\langle \mathbf{A} \rangle$ is a vector containing the occupacy probabilities with A's, $\mathbf{M}'$ is the matrix of coefficients, and $\mathbf{v}'$ is the vector that makes this systems nonhomogeneous having nonzero elements for indices 1 and S. We substitute $\langle \mathbf{A} \rangle = \langle \mathbf{A} \rangle_{ss} + \mathbf{c}$ in the rate equations (A1), where $\mathbf{c}$ is the vector with the deviations of the site occupancy probabilities with A's from the steady state. The substitution yields

$$\frac{d\mathbf{c}}{dt} = \mathbf{M}'[\langle \mathbf{A} \rangle_{ss} + \mathbf{c}] + \mathbf{v}' = \mathbf{M}'\mathbf{c} + \mathbf{M}'\langle \mathbf{A} \rangle_{ss} + \mathbf{v}' = \mathbf{M}'\mathbf{c},$$

$$(45)$$

because $\mathbf{M}'\langle \mathbf{A} \rangle_{ss} + \mathbf{v}' = 0$ by definition.

The equations in $\mathbf{c}$ are homogeneous and the matrix of coefficients is the same as the one in the original rate equations. We can obtain the eigenvalue equation by making the substitution

$$\mathbf{c} = \mathbf{c}' e^{-\omega t} \qquad (46)$$

and taking out the exponential from the equations. The relaxation time of the A loading (Q_A) is then the reciprocal of the smallest eigenvalue. We can get this time by simply numerically solving the eigenvalue equation.
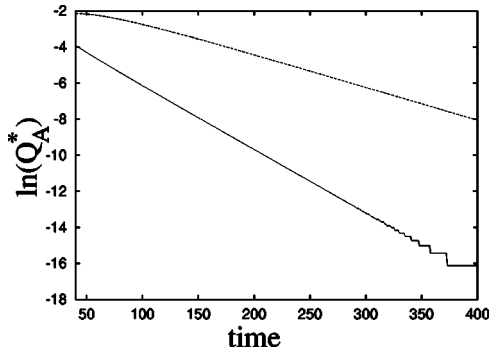
FIG. 6. Time dependences for $\ln(Q_A*)$ for a slow reaction system ($W_{ads}=0.8, W_{des}=0.2, W_{rx}=0.1, W_{diff}=2, S=30$) in the reaction limited regime when a number of ten reactive sites are homogeneously distributed in the system. The continous line is for the numerical results obtained solving the eigenvalue equation of the system in the reaction limited regime, and the dashed line is for the MF results. We have marked with * the difference between the current value and the steady-state value of the parameter.

Solving the eigenvalue equation for the case with conversion

For fast reaction systems we have seen that using MF, the A and B loadings have the same relaxation, which is the relaxation of the total loading Q [see Fig. 4(a)]. The relaxation of Q_A can be thus derived from exact equations (13) and (14). For slow reaction systems we can derive analytically the relaxation of Q_A and Q_B for the reaction limited regime. In this case we expect the relaxation of Q_A and Q_B to be determined only by reaction. From the MF results we remark that desorption has also a strong influence on the transients [see Fig. 4(c)]. This is happening because, in the case desorption is very high, the adsorbed particles at the marginal sites will hardly diffuse into the pipe, most of them being desorbed immediately. As a result, few particles will succeed in getting to the middle sites and the residence time of the particles near the marginal sites will decrease. The loading of the pipe with particles will converge slower to the steady state. We have compared also for different distributions of the reactive sites the results obtained solving the eigenvalue equation and the MF results for the system in the reaction limited regime. We find that if marginal sites are reactive the results are similar but differ considerably if the middle sites are reactive and for the homogeneous distribution of the reactive sites. In Fig. 6 we can see the difference between MF results and analytical results obtained solving the eigenvalue equation for the system in the reaction limited regime for the case when we have a homogeneous distribution of the reactive sites in the system.

Analytically, solving the eigenvalue equation for a very slow reaction system, we find that the relaxation of Q_A (t_{relA}) as a function of desorption varies with reaction for low desorption rates and converges to a limiting value for very high rates of desorption (see Fig. 7). The dependence of A loading on W_{des} has two regimes, the first for low desorption rates when A loading strongly decreases with desorption, and the second when the A loading is converging to a limiting value and the adsorption process takes over the system behavior.
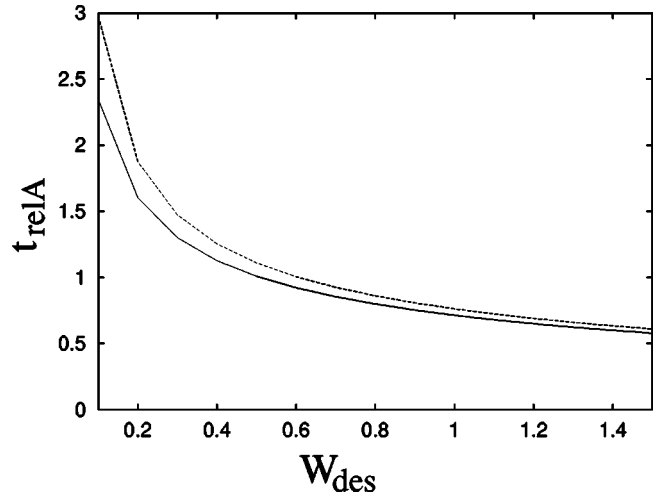

FIG. 7. The analytical results for the relaxation of Q_A as a function on W_{des} for different reaction rates. The continuous line is for $W_{rx}=0.1$ and the dashed line for $W_{rx}=0.01$, when $W_{des} \in [0,2]$.

We remark that the analytical results for Q_A obtained from the eigenvalue equation do not give the MF peak of A's particles accumulated in the transient regime for a slow reaction system (see Fig. 5).

C. Comparisons with simulation results

We present now the results obtained for the transients using DMC methods for different sets of parameters. We compare them with the mean-field and pair approximation results. As for very large pipes the computational effort is considerable, we study a system of size $S=30$. We have considered separately the sets of parameters in Table I.

The sets of parameters from (a) to (e) are for the cases of low loading and from (f) to (j) for high loading. The parameters in the table describe the following situations: (a) and (f) for very slow reaction and slow diffusion; (b) and (g) for
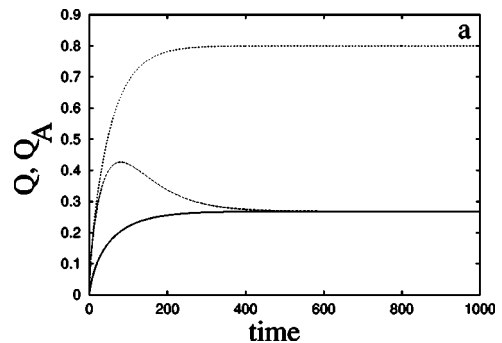

FIG. 5. (a) MF results (dashed line) and analytical results obtained solving the eigenvectors in the reaction limited regime (continuous line) for time dependence of Q_A for the parameters $W_{ads}=0.8, W_{des}=0.2, W_{rx}=0.01, W_{diff}=2.0, S=30$ and all the sites reactive. The upper dashed line represents the total loading (Q) in the system. The total loading Q gives us the information when the reaction limited regime starts.

TABLE I. The sets of parameters used for the simulations

Case	W_{ads}	W_{des}	W_{diff}	W_{rx}
(a)	0.2	0.8	0.05	0.01
(b)	0.2	0.8	0.05	0.1
(c)	0.2	0.8	2	0.1
(d)	0.2	0.8	1	2
(e)	0.2	0.8	10	2
(f)	0.8	0.2	0.05	0.01
(g)	0.8	0.2	0.05	0.1
(h)	0.8	0.2	2	0.1
(i)	0.8	0.2	1	2
(j)	0.8	0.2	10	2

FIG. 9. MF results for the time dependence of Q_A for $Q=0.2$, 0.5, 0.8, and $W_{rx}=0.01$.

slow reaction and slow diffusion; (c) and (h) for slow reaction and fast diffusion; (d) and (i) for fast reaction and slow diffusion; (e) and (j) for fast reaction and fast diffusion.

As the MF results for the total loading are exact, there are, as expected, no differences between these results and those of the simulation for the total loading. We compare the MF results with the simulation results for the case with conversion in the case all sites are reactive and also when only some of the sites are reactive.

1. All sites reactive

We first look at the time dependence of the loading with A (Q_A) and loading with B (Q_B). From the simulation results we see several regimes for the transients.

In the case diffusion is slow, the relaxation time is determined by diffusion. When diffusion is fast and the reaction slow, then the relaxation time is determined by reaction and when both are fast, relaxation time is determined by adsorption (desorption). For all these cases the simulations results for the transients match the MF results, except when we have low reaction rates and fast diffusion for both low and high loading (see Fig. 8).

When diffusion is fast and reaction is slow, MF overestimates the number of A's in the pipe both for transients and for the steady state. DMC and MF results indicate an overshoot for Q_A both for high and low loadings in the transient regime. The overshooting appears as a consequence of the difference the between diffusion and reaction rates constants.

Because the reaction is slow and diffusion fast, many A's start accumulating into the system and they are only later converted into B's. The moment t_{max} when the peak appears is determined by the ratio between W_{diff} and S, but always shortly after the initial moment t_0 and it lasts only a short time. The height of the peak depends on the total loading (W_{ads}/W_{des}) (see Fig. 9) and on the ratio between W_{rx} and W_{diff} (see Figs. 10 and 11). For the case of slow reaction and fast diffusion (f), (g), (h) in Table II, the higher the peak, the lower the ratio between W_{rx} and W_{diff}. In Table II we give the relative height of the peak ($\Delta H/Q_A$) for different W_{rx} and W_{diff}, at high loading ($W_{ads}=0.8, W_{des}=0.2$), where ΔH is the height of the peak.

MF overestimates the height of this peak comparing with simulation results, but both DMC and MF results converge in the same way to the steady state. In Fig. 12 we show that MF results corresponds to DMC results for transients for slow reaction systems. When diffusion is slow and reaction is fast, MF predicts very well the DMC results. We have also in this case an overshoot for Q_A in the transient regime. When we have slow diffusion and very slow reaction, the height of the peak increases with both W_{rx} and W_{diff} [see Table II for (d), (e), (f)]. Also in this case the MF corresponds to the DMC results.

As MF ignores the spatial correlations between NN sites and MF gives qualitatively good results comparing with DMC results, we conclude that MF is a good enough approximation for the case when all the sites are reactive. This is confirmed also by the comparison between MF and pair
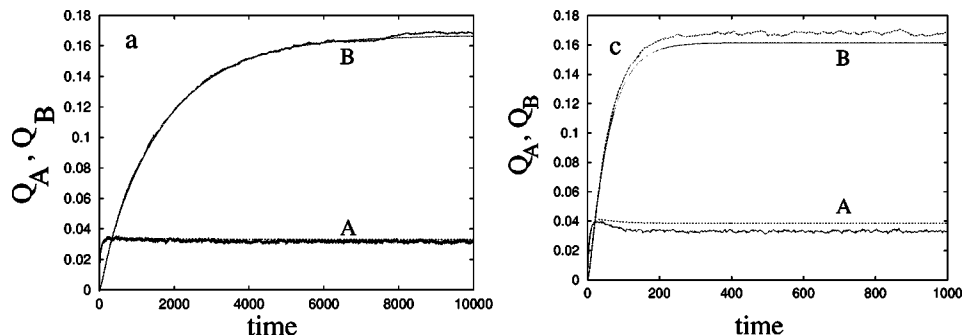

FIG. 8. DMC and MF results for the time dependences of Q_A and Q_B for the cases (a) and (c) in Table I when all the sites are reactive. Results for cases (b) and (f) are similar to (a) and results for case (h) are similar to case (c). The straight lines visible for case (c) (fast diffusion-slow reaction) are the MF lines. In the other cases the MF and the DMC results are indistinguishable.
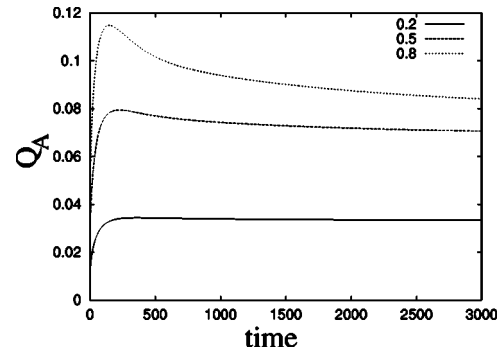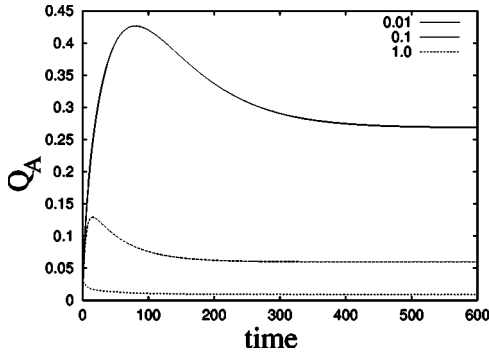
FIG. 10. MF results for the time dependence of Q_A for W_{rx} =0.01, 0.1, 1, when W_{ads}=0.8 and W_{des}=0.2.

TABLE II. The height of the peak for different W_{rx} and W_{diff}.

Case	W_{rx}	W_{diff}	$\Delta H/Q_A$	
			MF	Sim
(a)	0.01	2.0	1.5905	2.9521
(b)	0.1	2.0	2.1590	2.693
(c)	1.0	2.0	2.9911	2.9984
(d)	0.01	0.05	1.4365	1.2761
(e)	0.01	0.1	1.5070	1.4546
(f)	0.01	1.0	1.6458	2.654
(g)	0.01	2.0	1.5904	2.9384
(h)	0.01	10.0	1.4095	3.141
(i)	2.0	2.0	3.329	3.305

approximation. The pair approximation gives the same results as MF.

2. Only some of the sites reactive

We want to see how the distribution of the reactive sites influences the relaxation of A and B loadings. We compare the MF and the DMC results for fast reaction and for slow reaction systems, for different distributions of the reactive sites. We distinguish homogeneous distribution of the reactive sites, marginal sites reactive, and middle sites reactive.

We have previously seen that for fast reaction systems and all sites reactive, the relaxation of Q_A and Q_B is the same as the relaxation of the total loading Q. From Ref. [17] we know that the results for the total loading, both for transients and for the steady state, can be derived analytically from exact equations and these results corresponds to the DMC results. When only the marginal sites are reactive and reaction very fast, DMC and MF results are similar with DMC and MF results for the cases when all sites are reactive and when it is a homogeneous distribution of the reactive sites in the pipe. When the reactive sites are situated in the middle of the pipe, the loadings Q, Q_A, and Q_B relax slower to equilibrium than in the case wherein all the sites are reactive, because it takes more time for the A particles to reach the reactive sites.

For slow reaction systems and all sites reactive, the relaxation of Q_A and Q_B is slower than the relaxation of the total loading Q. For this case we cannot derive Q_A from exact equations. The A loading is converging to equilibrium simul-
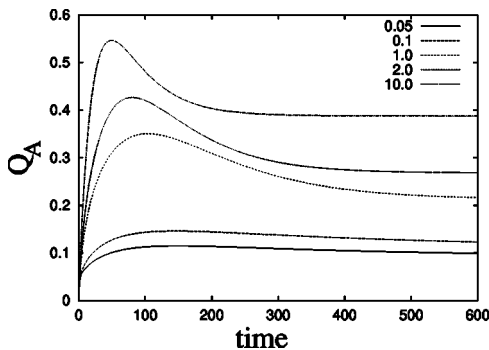
taneously with the B loading. We compare thus DMC and MF results for different distributions of the reactive sites, for different reaction rates. We will analyze two cases, the first for slow reaction (W_{rx}=0.1) and the second for very slow reaction (W_{rx}=0.01).

In the first case (W_{rx}=0.1), the B loading for homogenous distribution and middle site reactive reaches equilibrium faster than in the case when marginal sites are reactive. This is happening because for marginal sites reactive case, the B's are formed near the open ends and, consequently, they can easily desorb and the equilibrium is reached later. When the marginal sites are reactive, the residence time of the B's is small and the probability to find a B on a marginal site is high. The loading with B's is increasing more slowly to the steady state value because of the A's that are in the middle of the pipe. The same behavior has the A loading converging to equilibrium simultaneously with B loading. When the reactive sites are distributed in the middle of the pipe, because of blocking, the B's cannot reach easily the open ends, the probability to find a B on a marginal site is small, and the residence time of the B's in the system is large. The loading with B's is increasing fast to the steady state value. From Fig. 13, we see that Q_A and Q_B for homogeneous and middle sites reactive have the same relaxation.
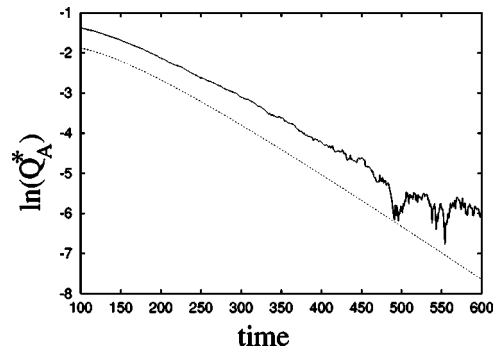

FIG. 12. Analytical and simulation results for slow reaction systems, W_{diff}=2, W_{rx}=0.1, W_{ads}=0.8, W_{des}=0.2, when all the sites are reactive. The simulation (continuous line) and analytical (dotted line) results for the $\ln(Q_A*)$ as a function of time. We have marked with * the difference between the current value and the steady-state value of Q_A.
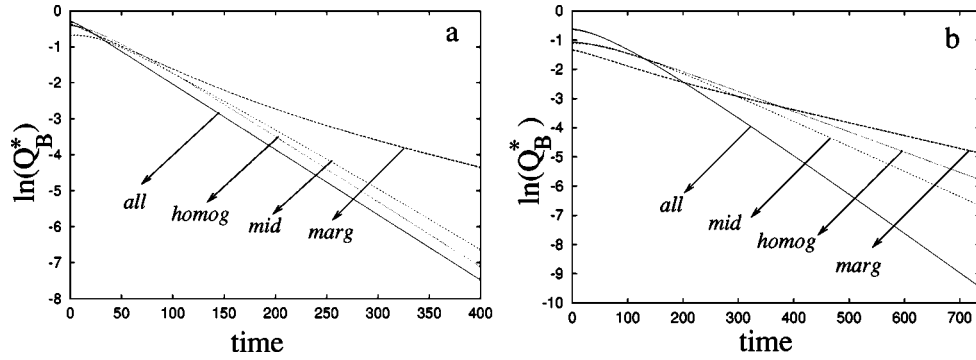

FIG. 11. MF results for the time dependence of Q_A for W_{diff} =0.05, 0.1, 1, 2, 10, when W_{ads}=0.8, W_{des}=0.2, W_{rx}=0.01.

FIG. 13. (a) Time dependences for $\ln(Q_B*)$ when $W_{ads}=0.8$, $W_{des}=0.2$, $W_{diff}=2$, $W_{rx}=0.1$ using MF for marginal sites reactive, homogeneous distribution, middle sites reactive, and all sites reactive cases. (b) Time dependences for $\ln(Q_B*)$ when $W_{ads}=0.8$, $W_{des}=0.2$, $W_{diff}=2$, $W_{rx}=0.01$ using MF for the same distributions of the reactive sites as in (a). In (a) and (b) we have marked with * the absolute value of the difference between the current value and the steady-state value of the parameter.

In the case of very slow reaction ($W_{rx}=0.01$), when the marginal sites are reactive, the B loading increases faster than in the case of homogeneous and middle sites reactive, till a certain time because A particles can reach faster the reactive sites. While more B's are formed, the B loading is converging slower because the B's can desorb relatively fast from the marginal sites, the residence time of the formed B's is smaller than in the case when the reactive sites are in the middle of the pipe or homogeneously distributed (see Fig. 13). Q_B converges faster in case the middle sites are reactive than in the case of homogeneous distribution of the reactive sites.

We compare the time dependence of the A loading and of the B loading using DMC and MF for slow reaction systems and different rates of conversion when diffusion is fast (see Fig. 14). We see that differences appear in the transient region as well as in the steady state for all the distributions of the reactive sites but are very prominent for the marginal and middle sites reactive case. In this case, for homogeneous distribution of the reactive sites the differences between MF and DMC are small (see Fig. 15).

For the other cases (fast reaction–slow diffusion, fast reaction–fast diffusion, slow reaction–slow diffusion), MF gives good results compared to DMC for all the distributions of the reactive sites.

We finally look at the site occupancy of the pipe. The MF profiles for the marginal sites reactive case show in the transient regime accumulation of the A's in the middle of the pipe for a slow reaction system and fast diffusion. Because reaction is slow, the A's can pass without reacting to the nonreactive sites. As the loading is increasing, the residence time of the particles increases, and the probability to find an A in the middle of the pipe decreases because of blocking (see Fig. 16).

Dynamic Monte Carlo simulations show the same behavior. In Fig. 17 we see as well accumulation of A particles in the middle of the pipe in the transient regime. As a consequence, until the equilibrium is reached, the middle sites have different contribution to the occupancy in the pipe depending on their position. In the steady state, all the middle sites have the same contribution to the occupancy profiles [17].

IV. SUMMARY

We have used DMC and analytical techniques to study the properties of single-file systems in the transient regime.

We have derived exact equations to solve the relaxation time of the whole system (t_{rel}). We found that there are two regimes describing the dependence on diffusion of the relax-
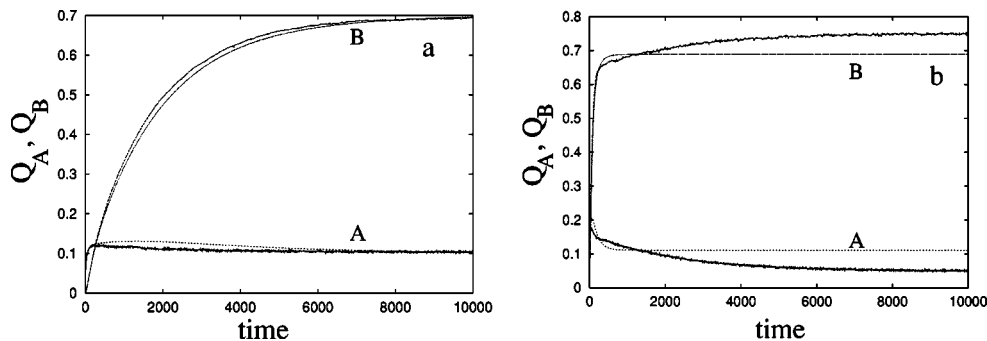

FIG. 14. (a) DMC simulation of time dependences for Q_A and Q_B for $W_{ads}=0.8, W_{des}=0.2, W_{diff}=0.05, W_{rx}=0.01$, when blocks of five marginal sites are reactive ($S=30$). The straight lines correspond to the MF results. (b) DMC simulation of time dependences for Q_A and Q_B for $W_{ads}=0.8, W_{des}=0.2, W_{diff}=2, W_{rx}=0.1$, when blocks of five marginal sites are reactive ($S=30$). The straight lines correspond to the MF results.
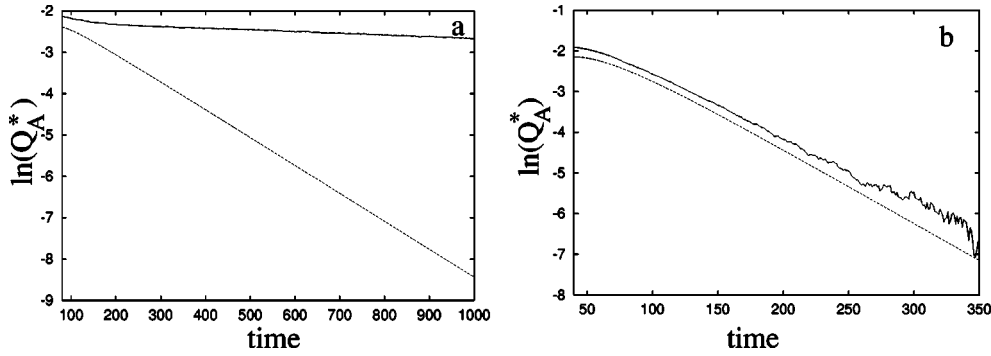
FIG. 15. (a) Time dependences for $\ln(Q_A*)$ for a slow reaction system ($W_{ads}=0.8$, $W_{des}=0.2$, $W_{rx}=0.1$, $W_{diff}=2$, $S=30$) when five left and right marginal sites are reactive. (b) Time dependences for $\ln(Q_A*)$ for a slow reaction system ($W_{ads}=0.8$, $W_{des}=0.2$, $W_{rx}=0.1$, $W_{diff}=2$, $S=30$) when ten reactive sites are homogeneously distributed in the system. In (a) and (b) the continuous line is for the DMC results and the dashed line is for the MF results. We have marked with * the difference between the current value and the steady-state value of the parameter.

ation time t_{rel}. The first regime is for slow diffusion, when t_{rel} decreases fast with increasing diffusion, and the second for fast diffusion, when t_{rel} slowly decreases with diffusion to a limiting value. We have analytically derived this limiting value of t_{rel} for infinitely fast diffusion.

We have also studied the transients in the case with conversion. MF results show that there are two different behaviors determined by conversion. For fast reaction systems, the relaxation time of the loading with A's (t_{relA}) and B's (t_{relB}) is equal to the relaxation time of the total loading (t_{rel}). When Q has reached equilibrium, Q_A and Q_B have also reached equilibrium. For slow reaction systems, the total loading Q relaxes faster to equilibrium than the loading with A's (Q_A) and B's (Q_B). The regime between Q reaching equilibrium and Q_A and Q_B reaching equilibrium we call the reaction limited regime. In the reaction limited regime, MF shows that not only reaction, but also desorption has a strong influence influence on the transients. We find that the relaxation of Q_A (t_{relA}) as a function of desorption varies with reaction for low desorption rates and converges to a limiting

value for very high rates of desorption.

DMC results show several regimes for the transients, in the case all the sites are reactive. In the case diffusion is slow, the relaxation time is determined by diffusion. When diffusion is fast and the reaction slow, then the relaxation time is determined by reaction and when both are fast, relaxation time is determined by adsorption (desorption). For all these cases the simulations results for the transients match the MF results, except when we have low reaction rates and fast diffusion for both low and high loading. In this case MF overestimates the amount of A's in the pipe both for transients and for the steady state. DMC and MF results indicate also an overshoot for Q_A both for high and low loadings in the transient regime, which appears as a consequence of the difference between diffusion and reaction rates constants.

When only some of sites are reactive, for fast reaction systems, MF gives good results compared to DMC for all the distributions of the reactive sites. When only the marginal sites are reactive and reaction very fast, DMC and MF results are similar with DMC and MF results for the cases when all
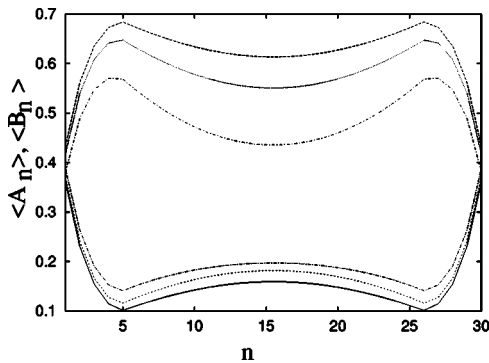

FIG. 16. MF profile occupancies ($\langle A_n \rangle$ and $\langle B_n \rangle$) for the case of five marginal sites reactive before a steady state is reached for a slow reaction system of length $S=30$ and parameters $W_{ads}=0.8$ and $W_{des}=0.2$, $W_{diff}=2$, $W_{rx}=0.1$. The lines at low occupancies correspond to $\langle A_n \rangle$ profile occupancies after 200, 150, and 100 time units in this order from the bottom to the top. The lines at high occupancies correspond to $\langle B_n \rangle$ profile occupancies after 200, 150, and 100 time units in this order from the top to the bottom.
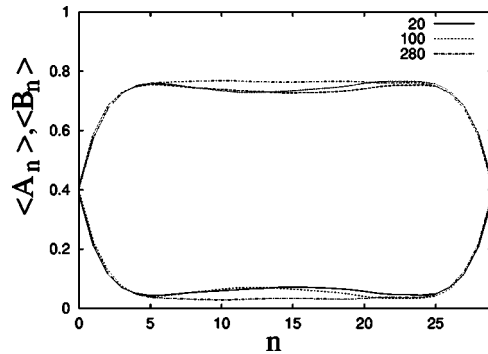

FIG. 17. DMC results for the occupancy profiles ($\langle A_n \rangle$ and $\langle B_n \rangle$) for slow reaction systems ($W_{ads}=0.8$, $W_{des}=0.2$, $W_{diff}=2$, $W_{rx}=0.1$) in the case five marginal sites are reactive, before steady state is reached. The lines at low occupancies correspond to $\langle A_n \rangle$ profile occupancies after 280, 100, and 20 time units in this order from the bottom to the top. The lines at high occupancies corresponds to $\langle B_n \rangle$ profile occupancies after 280, 100, and 20 time units in this order from the top to the bottom.

sites are reactive and when it is a homogeneous distribution of the reactive sites in the pipe. When the reactive sites are situated in the middle of the pipe, the loadings Q, Q_A, and Q_B relax slower to equilibrium than in the case when all the sites are reactive, because it takes more time for the A particles to reach the reactive sites.

For slow reactive systems, differences between DMC and MF results appear for transients for different distributions of the reactive sites when diffusion is fast, but are very prominent for marginal and middle sites reactive. For homogeneous distribution of the reactive sites the differences between MF and DMC are small. For slow reaction, we find that the B loading for homogenous distribution and middle site reactive reaches equilibrium faster than in the case of when marginal sites is reactive. For very slow reaction, Q_B increases faster at the beginning than in the case of homogeneous and middle sites reactive and becomes slower as the B's are formed. Q_B converges also faster in the case the middle sites are reactive than in the case of homogeneous distribution of the reactive sites.

ACKNOWLEDGMENT

The authors thank Professor R. A. van Santen for many stimulating discussions.

APPENDIX

Derivation of the equations for two-sites probabilities

In order to solve the rate equations of the system we use cluster approximation. For simplicity, we consider an approximation that considers only the correlations between pairs of NN sites—pair approximation. We add the two-site probability equations to the already derived rate equations for one-site probabilities. We write these equations in terms of three-site probabilities and we use then the decoupling scheme

$$\langle XYZ \rangle = \frac{\langle XY \rangle \langle YZ \rangle}{\langle Y \rangle}. \tag{A1}$$

We give here the equations for the two-site probabilities for A and $*$ occupancy of these sites. The equations for the left marginal sites are

$$\frac{d\langle A_1 A_2 \rangle}{dt} = W_{\text{diff}}(\langle A_1 *_2 A_3 \rangle - \langle A_1 A_2 *_3 \rangle) - 2W_{\text{rx}}\langle A_1 A_2 \rangle$$
$$+ W_{\text{ads}}\langle *_1 A_2 \rangle - W_{\text{des}}\langle A_1 A_2 \rangle,$$

$$\frac{d\langle A_1 *_2 \rangle}{dt} = W_{\text{diff}}(\langle *_1 A_2 \rangle + \langle A_1 A_2 *_3 \rangle + \langle A_1 B_2 *_3 \rangle - \langle A_1 *_2 \rangle$$
$$- \langle A_1 *_2 A_3 \rangle - \langle A_1 *_2 B_3 \rangle) - W_{\text{rx}}\langle A_1 *_2 \rangle$$
$$+ W_{\text{ads}}\langle *_1 *_2 \rangle - W_{\text{des}}\langle A_1 *_2 \rangle$$

$$\frac{d\langle *_1 A_2 \rangle}{dt} = W_{\text{diff}}(\langle A_1 *_2 \rangle + \langle *_1 *_2 A_3 \rangle - \langle *_1 A_2 \rangle - \langle_1 * A_2 *_3 \rangle)$$
$$- W_{\text{rx}}\langle *_1 A_2 \rangle - W_{\text{ads}}\langle *_1 A_2 \rangle + W_{\text{des}}(\langle A_1 A_2 \rangle$$
$$+ \langle B_1 A_2 \rangle),$$

$$\frac{d\langle_1 * *_2 \rangle}{dt} = W_{\text{diff}}(\langle_1 * A_2 *_3 \rangle + \langle_1 * B_2 *_3 \rangle - \langle_1 * *_2 A_3 \rangle$$
$$- \langle_1 * *_2 B_3 \rangle) - W_{\text{ads}}\langle_1 * *_2 \rangle + W_{\text{des}}(\langle A_1 *_2 \rangle$$
$$+ \langle B_1 *_2 \rangle), \tag{A2}$$

where $\langle A_1 *_2 A_3 \rangle = \langle A_1 *_2 \rangle \langle A_2 *_3 \rangle / \langle_2 * \rangle$, etc. Almost similar are the equations for the right marginal sites

$$\frac{d\langle A_{S-1} A_S \rangle}{dt} = W_{\text{diff}}(\langle A_{S-2} *_{S-1} A_S \rangle - \langle_{S-2} * A_{S-1} A_S \rangle)$$
$$- 2W_{\text{rx}}\langle A_{S-1} A_S \rangle + W_{\text{ads}}\langle A_{S-1} *_S \rangle$$
$$- W_{\text{des}}\langle A_{S-1} A_S \rangle,$$

$$\frac{d\langle A_{S-1} *_S \rangle}{dt} = W_{\text{diff}}(\langle A_{S-1} *_S *_{S+1} \rangle + *_{S-1} A_S \rangle - \langle A_{S-1} *_S \rangle$$
$$- \langle_{S-2} * A_{S-1} *_S \rangle) - W_{\text{rx}}\langle A_{S-1} *_S \rangle$$
$$- W_{\text{ads}}\langle A_{S-11} *_S \rangle + W_{\text{des}}(\langle A_{S-1} A_S \rangle$$
$$+ \langle A_{S-1} B_S \rangle),$$

$$\frac{d *_{S-1} A_S \rangle}{dt} = W_{\text{diff}}(\langle A_{S-1} *_S \rangle + \langle_{S-2} * A_{S-1} A_S \rangle$$
$$+ \langle_{S-2} * B_{S-1} A_S \rangle - *_{S-1} A_S \rangle - \langle A_{S-2} *_{S-1} A_S \rangle$$
$$- \langle B_{S-2} *_{S-1} A_S \rangle) - W_{\text{rx}} *_{S-1} A_S \rangle$$
$$+ W_{\text{ads}}\langle *_{S-1} *_S \rangle - W_{\text{des}} *_{S-1} A_S \rangle,$$

$$\frac{d\langle_{S-1} * *_S \rangle}{dt} = W_{\text{diff}}(\langle_{S-2} * A_{S-1} *_S \rangle + \langle_{S-2} * B_{S-1} *_S \rangle$$
$$- \langle A_{S-2} *_{S-1} *_S \rangle - \langle B_{S-2} *_{S-1} *_S \rangle)$$
$$- W_{\text{ads}}\langle_{S-1} * *_S \rangle + W_{\text{des}}(*_{S-1} A_S \rangle$$
$$+ \langle *_{S-1} B_S \rangle). \tag{A3}$$

And, finally, the equations for the nonmarginal sites;

$$\frac{d\langle A_n A_{n+1}\rangle}{dt} = W_{\text{diff}}(\langle A_n *_{n+1} A_{n+2}\rangle + \langle A_{n-1} *_n A_{n+1}\rangle$$

$$- \langle A_{n-1} *_n A_{n+1}\rangle - \langle A_n A_{n+1} *_{n+2}\rangle)$$

$$- 2W_{\text{rx}}\langle A_n A_{n+1}\rangle,$$

$$\frac{d\langle A_n *_{n+1}\rangle}{dt} = W_{\text{diff}}(\langle A_n *_{n+1}\rangle + \langle A_{n-1} *_n *_{n+1}\rangle$$

$$+ \langle A_n A_{n+1} *_{n+2}\rangle + \langle A_n B_{n+1} *_{n+2}\rangle - \langle A_n *_{n+1}\rangle$$

$$- \langle A_n *_{n+1} A_{n+2}\rangle - \langle A_n *_{n+1} B_{n+2}\rangle$$

$$- \langle A_{n-1} *_n *_{n+1}\rangle) - W_{\text{rx}}\langle A_n *_{n+1}\rangle,$$

$$\frac{d\langle A_n *_{n+1}\rangle}{dt} = W_{\text{diff}}(\langle A_n *_{n+1}\rangle + \langle *_{n+1} A_{n+2}\rangle$$

$$+ \langle A_{n-1} *_n A_{n+1}\rangle + \langle *_{n-1} B_n A_{n+1}\rangle - \langle A_n *_{n+1}\rangle$$

$$- \langle A_n *_{n+1} *_{n+2}\rangle - \langle A_{n-1} *_n A_{n+1}\rangle$$

$$- \langle B_{n-1} *_n A_{n+1}\rangle) - W_{\text{rx}}\langle A_n *_{n+1}\rangle,$$

$$\frac{d\langle *_n *_{n+1}\rangle}{dt} = W_{\text{diff}}(\langle A_n *_{n+1} *_{n+2}\rangle + \langle B_n *_{n+1} *_{n+2}\rangle$$

$$+ \langle A_{n-1} *_n *_{n+1}\rangle + \langle *_{n-1} B_n *_{n+1}\rangle$$

$$- \langle *_n *_{n+1} A_{n+2}\rangle - \langle *_n *_{n+1} B_{n+2}\rangle$$

$$- \langle A_{n-1} *_n *_{n+2}\rangle - \langle B_{n-1} *_n *_{n+1}\rangle). \quad \text{(A4)}$$

We have the possibility to determine the one-site probabilities by calculating the sum of the two-sites probabilities $\Sigma_Y \langle XY\rangle = \langle X\rangle$.

[1] R.J. Baxter, *Exactly Solved Models in Statistical Mechanics* (Academic Press, New York, 1982).

[2] B. Derrida and M. Evans, *Nonequilibrium Statistical Mechanics in One Dimension*, edited by V. Privman (Cambridge University Press, Cambridge, 1997).

[3] F.C. Alcaraz, Int. J. Mod. Phys. B **8**, 3349 (1994).

[4] B. Derrida, E. Domany, and D. Mukamel, J. Stat. Phys. **69**, 667 (1992).

[5] G. Schutz and E. Domany, J. Stat. Phys. **72**, 277 (1993).

[6] B. Derrida, M.R. Evans, V. Hakim, and V. Pasquier, J. Phys. A **26**, 1493 (1993).

[7] J.G. Tsikoyannis and J. Wei, Chem. Eng. Sci. **46**, 233 (1991).

[8] C. Rödenbeck, J. Kärger, and K. Hahn, Phys. Rev. E **55**, 5697 (1997).

[9] M.S. Okino, R.Q. Snurr, H.H. Kung, J.E. Ochs, and M.L. Mavrovouniotis, J. Chem. Phys. **111**, 2210 (1999).

[10] M.-O. Coppens, A. Bell, and Chakraborty, Chem. Eng. Sci. **53**, 2053 (1998).

[11] M.-O. Coppens, A. Bell, and Chakraborty, Chem. Eng. Sci. **54**, 3455 (1999).

[12] V. Privman, *Nonequilibrium Statistical Mechanics in One Dimension* (Cambridge University Press, Cambridge, 1997).

[13] J. Marro and R. Dickman, *Nonequilibrium Phase Transitions in Lattice Models* (Cambridge University Press, Cambridge, 1998).

[14] R. Dickman and I. Jensen, Phys. Rev. Lett. **67**, 2391 (1991).

[15] G. Grinstein, Z.W. Lai, and D.A. Browne, Phys. Rev. A **40**, 4820 (1989).

[16] R. Dickman and M. Burschka, Phys. Lett. A **127**, 132 (1988).

[17] S.V. Nedea, A.P.J. Jansen, J.J. Lukkien, and P.A.J. Hilbers, Phys. Rev. E (to be published).

[18] B. Derrida and M.R. Evans, J. Phys. A **32**, 4833 (1999).

[19] E. Ben-Naim and P.L. Krapivsky, J. Phys. A **27**, 481 (1994).

[20] B. Derrida, V. Hakim, and R. Zeitak, Phys. Rev. Lett. **77**, 2871 (1996).

[21] J. Mai, V. Kuzovkov, and W. von Niessen, J. Chem. Phys. **100**, 8522 (1994).

[22] M. von Smoluchowski, Z. Phys. Chem. **92**, 129 (1917).

[23] V. Kampen, *Stochastic Processes in Physics and Chemistry* (Elsevier Science, Amsterdam, 1981).

[24] H. Mamada and F. Takano, J. Phys. Soc. Jpn. **25**, 675 (1968).

[25] J. Lukkien, J. Segers, P.A.J. Hilbers, R.J. Gelten, and A.P.J. Jansen, Phys. Rev. E **58**, 2598 (1998).

[26] R.J. Gelten, A.P.J. Jansen, R. van Santen, J.J. Lukkien, and P. Hilbers, J. Chem. Phys. **108**, 5921 (1998).

[27] R.J. Gelten, R. van Santen, and A.P.J. Jansen, in *Dynamic Monte Carlo Simulations of Oscillatory Heterogeneous Catalytic Reactions,* edited by P.B. Balbuena and J.M. Seminario (Elsevier, Amsterdam, 1999).

[28] R.J. Gelten, R. van Santen, and A.P.J. Jansen, Isr. J. Chem. **38**, 415 (1998).

[29] A.P.J. Jansen, Comput. Phys. Commun. **86**, 1 (1995).

[30] J. Segers, Ph.D. thesis, Eindhoven University of Technology, 1999.

[31] K. Binder, *Monte Carlo Methods in Statistical Physics* (Springer, Berlin, 1986).

[32] D. Gillespie, J. Comput. Phys. **22**, 403 (1976).

[33] D. Gillespie, J. Phys. Chem. **81**, 2340 (1977).

[34] J. Mai, V. Kuzovkov, and W. von Niessen, J. Chem. Phys. **100**, 6073 (1994).

[35] A.J. Guttmann, *Asymptotic Analysis of Power-Series Expansions in Phase Transitions and Critical Phenomena* (Academic Press, New York, 1989).

[36] D.J. Amit, *Field Theory, The Renormalization Group, and Critical Phenomen* (World Scientific, Singapore, 1984).

[37] T.M. Liggett, *Interacting Particle Systems* (Springer, Berlin, 1985).

[38] H. Spohn, *Interacting Particle Systems* (Springer, Berlin, 1991).

[39] B.M. McCoy and T.T. Wu, *The Two-Dimensional Ising Model*

(Harvard University Press, Cambridge, 1973).

[40] A.M. Polyakov, Pis'ma Zh. Eksp. Teor. Fiz. **12**, 538 (1970) [Sov. Phys. JETP **12**, 381 (1970)].

[41] J.L. Cardy, *Phase Transitions and Critical Phenomena* (Academic Press, New York, 1987).

[42] M. Henkel, *Conformal Invariance and Critical Phenomena* (Springer Verlag, Berlin, 1999).

[43] B. Schmittmann and R.K.P. Zia, *Statistical Mechanics of Driven Diffusive Systems in Phase Transitions and Critical*

phenomen (Academic Press, New York, 1995).

[44] F.C. Alcaraz, M.H.M. Droz, and V. Rittenberg, Ann. Phys. (N.Y.) **230**, 250 (1994).

[45] M.R. Evans, N. Rajewsky, and E.R. Speer, J. Stat. Phys. **95**, 45 (1999).

[46] L.H. Gwa and H. Spohn, Phys. Rev. A **46**, 844 (1992).

[47] C.R. Doering, M.A. Burschka, and W. Horsthemke, J. Stat. Phys. **65**, 953 (1991).